Int. J. Heat Mass Transfer. Vol. 28, No. 9, pp. 1757–1771, 1985
Printed in Great Britain

0017-9310/85 $3.00 + 0.00

Wall independency and effect of initial shear-layer thickness in separated flow and heat transfer

WIN AUNG
National Science Foundation, Washington, DC 20550, U.S.A.

and

AMICHAI BARON and FU-KANG TSOU
Department of Mechanical Engineering and Mechanics, Drexel University, Philadelphia, PA 19104, U.S.A.

(*Received* 27 *August* 1984 *and in final form* 6 *March* 1985)

Abstract—Theoretical results are presented concerning the flow and heat transfer in laminar flow past a backstep. Computations are carried out using the stream function–vorticity forms of the elliptic partial differential equations. The effects of step size and initial boundary-layer thickness are discussed, and calculated temperature profiles and local Stanton numbers are compared with recently reported experimental data. It is shown that the size of the initial boundary layer can have opposing effects on the reattachment distance, depending on whether the Reynolds number is held constant. The influence on the average heat transfer of the flow and thermal structures in the reversed flow region is assessed by comparing the numerical solutions with the solutions for the wall-independent shear layer.

INTRODUCTION

RECENT developments in high performance heat exchangers and in the cooling of electronic equipment have led to a need for more quantitative information on heat transfer rates in separated flow regions. The present paper concerns the particular type of two-dimensional separated flow that is associated with a plane flow past a backstep. While there are several flow phenomena that are of interest, here we deal with the fully laminar situation in which not only the flow approaching the step is laminar, but the flow in the separated region as well as in the reattached, redeveloping boundary layer is laminar. In addition, the plate upstream of the step is considered to have a finite length so that the boundary thickness at the step becomes a parameter that must be reckoned with.

Reported studies for backstep flows predominantly deal with turbulent flow [1]; however, in the aforementioned applications, the fluid velocities and/or the channel dimensions are small, and hence laminar flow is important. In laminar flow, the available results indicate that the shear-layer reattachment length, when normalized by the step height, increases with the Reynolds number in the range $25 < Re_s < 850$. As the Reynolds number increases above a value of approx. 850, transition to turbulence occurs in the shear layer starting at a location near the reattachment point. In the beginning stages of transition, the normalized reattachment length continues to increase with Re_s, but the rate of increase is appreciably reduced. At still higher values of the Reynolds number, an opposite trend sets in as the normalized reattachment distance decreases with an increase of the Reynolds number. Yet another phenomenon enters the picture when the flow is fully turbulent, that is, when the boundary layer approaching the step is turbulent and the entire shear layer is turbulent. In this case, the normalized reattachment distance attains a relatively constant value that nevertheless appears to vary from one study to another.

In a recent paper, Aung [2] presented heat transfer measurements for laminar flow past backsteps where the step walls are maintained at a constant temperature. Results are given for the local heat transfer as well as the average value in the separated regions. It was found in [2] that the average Stanton number exhibits a minus one-half power dependency on the Reynolds number. This relationship is in agreement with the wall-independent, thin shear-layer analysis originally formulated for high speed, laminar flow with vanishing initial shear-layer thickness [3]. The experimental data show that as the step size decreases, and hence the relative magnitude of the initial shear-layer thickness becomes larger, the heat transfer in the separated region is depressed although the minus one-half power relationship is preserved. Since the wall-independent shear-layer analysis has been successful in precisely predicting the experimental data at least in one case it seems worthwhile to examine further the fundamental properties of the analysis of backstep flow, and to observe how they relate to each other.

In addition to the above, it is also noted that the experimental results have not provided a satisfactory

NOMENCLATURE

L reattachment distance
Nu Nusselt number, hs/k
Re_s Reynolds number, $\rho Us/\mu$
s step height
Re_{x_s} Reynolds number, $\rho U x_s/\mu$
St Stanton number, $h/(\rho c_p U)$
T temperature
U free-stream velocity (Fig. 1a)
x_s defined in Fig. 1a.

Greek symbols
α thermal diffusivity
β residue defined in equation (6)
δ boundary-layer thickness
δ^* displacement thickness
ξ distance from the step (Fig. 1a)
ψ stream function defined in equation (2)
ω vorticity defined in equation (3).

Subscripts
FP condition for flat plate.

explanation regarding the role of the initial shear layer in separated forced convection. The results in [2] indicate a relatively strong effect of the initial shear-layer thickness on the average heat transfer. By contrast, the initial shear-layer thickness has a rather mild influence on the average heat transfer in the case of laminar flow past cavities [4]. Since the heat transfer in separated forced convection is effected primarily through a vortex flow mechanism, it becomes of interest to examine how the strength of the vortices in the separated flow region depend on the initial boundary-layer thickness. There has been no report of such a study in the literature. In view of recent advances in computational capability, this problem can be studied advantageously by employing numerical methods and this forms a second objective in the present investigation. A vorticity–stream function formulation is employed herein, so as to provide the necessary detail for the flowfield.

In the course of this study, a theoretical study of forced convection in laminar flow past rearward-facing steps was reported by Hall and Fletcher *et al.* [5]. The method employed by these investigators is based on an interaction model that combines boundary-layer theory with an inviscid flow calculation. They show that the method is capable of reproducing some of the experimental data reported in [2].

MATHEMATICAL TECHNIQUES

Differential equations

Consider an incompressible, two-dimensional laminar flow. The conservation equations of the elliptic type which govern the stream function (ψ), the vorticity (ω), and the temperature (T) in Cartesian coordinates can be written as [6],

$$a\left[\frac{\partial}{\partial x}\left(\phi\frac{\partial\psi}{\partial y}\right)-\frac{\partial}{\partial y}\left(\phi\frac{\partial\psi}{\partial x}\right)\right]-\frac{\partial}{\partial x}\left[b\frac{\partial(c\phi)}{\partial x}\right]-\frac{\partial}{\partial y}\left[b\frac{\partial(c\phi)}{\partial y}\right]+S=0 \quad (1)$$

Table 1. The functions a, b, c and S

ϕ	a	b	c	S
ω	1	1	μ	0
ψ	0	$1/\rho$	1	$-\omega$
T	1	$\rho\alpha$	1	0

where ϕ stands for any one of the unknowns ψ, ω and T.

The functions a, b, c and S, are given in Table 1.

The definitions of ψ and ω are,

$$u=\frac{1}{\rho}\frac{\partial\psi}{\partial y},\quad v=-\frac{1}{\rho}\frac{\partial\psi}{\partial x}. \quad (2)$$

$$\omega=\frac{\partial v}{\partial x}-\frac{\partial u}{\partial y}. \quad (3)$$

Equations (1)–(3) and the boundary conditions described in the next paragraph are applied to the present back step problem (see Fig. 1a). The approaching boundary layer, flow separation, recirculation region and reattachment point are indicated in the figure. The whole flow field is considered to be laminar.

Boundary conditions

It is seen from Fig. 1a that heating starts at the location with the distance x_0 from the leading edge. The wall temperature (T_w) is kept constant for $x \geqslant x_0$. The area ABCDEF shown in Fig. 1b is used as the computational region whose sides are chosen as,

$$\text{AB} = 10s,$$

$$\text{CD} = 40s,$$

$$\text{DE} = 22s,$$

where s is the step height. The region is sufficiently large to give computational results that are size independent.

On the west boundary AF, the Blasius velocity and temperature profiles [7] are prescribed. The approaching length upstream of the step shown in Fig. 1a is

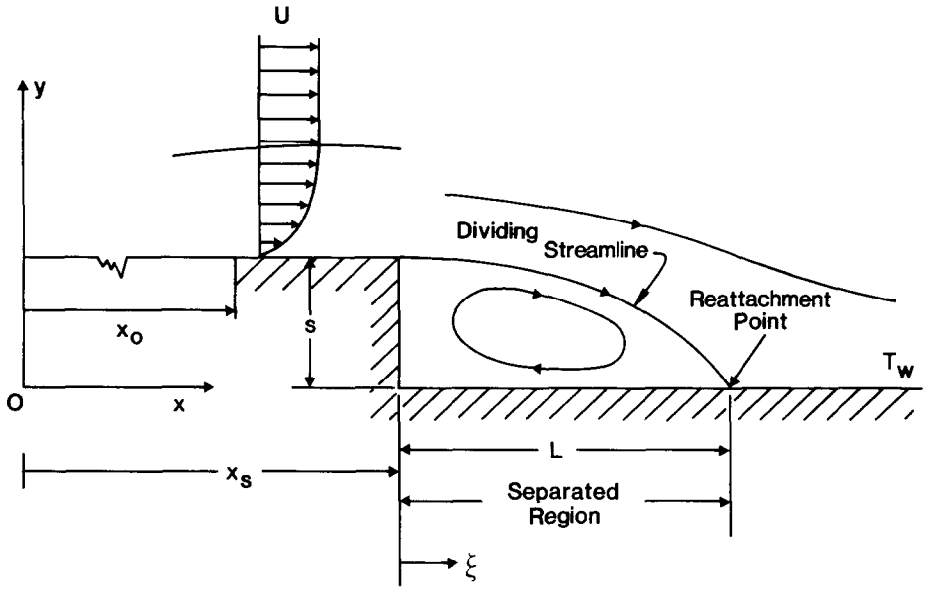

FIG. 1a. Flow over two-dimensional step.

chosen to conform with the experimental condition in [2]; i.e. $x_s = 45.5$ cm, and $x_o = 15.0$ cm in most computational cases. However in some other cases, x_o is arbitrarily changed in order to obtain different values of δ/s at the step, for a fixed value of Re_s. Since this approaching length is sufficiently long, one would expect that the streamlines above the surface AB (Fig. 1b) will be bent toward it resulting in a thinner boundary layer at the upper corner (point B). The present method thus provides for the streamline curvature effect noted in [2], wherein the effect has been observed to give a heat transfer augmentation at the step of as much as 30% when compared with attached flow.

Along the north boundary FE, constant free-stream velocity and temperature are prescribed. The east boundary DE is situated far away from the step. The property gradients along the streamwise direction are

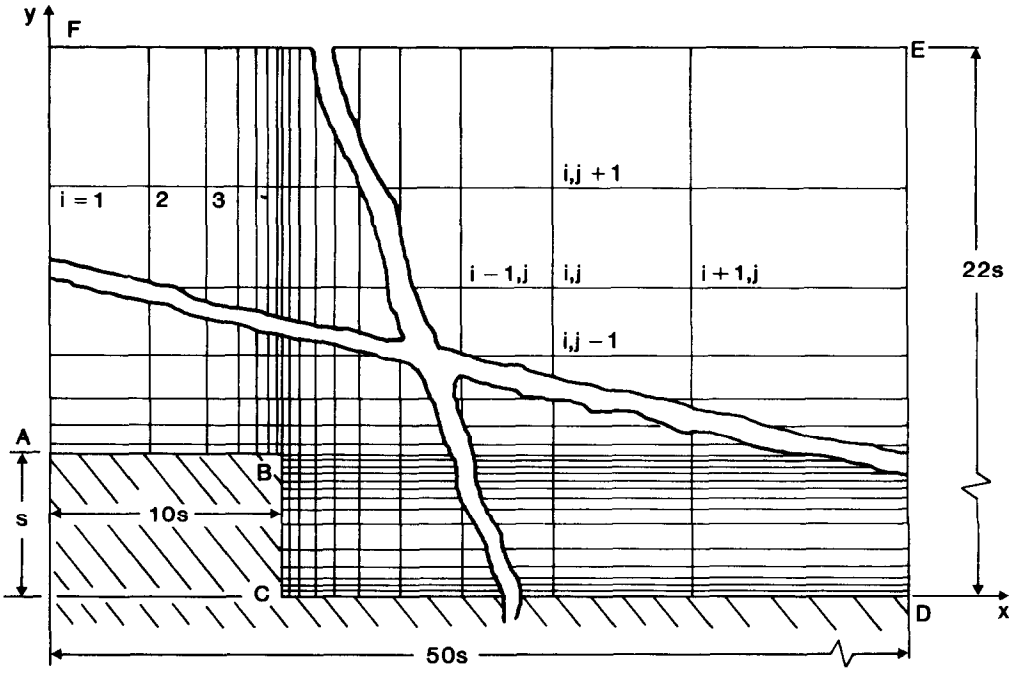

FIG. 1b. Non-uniform grid system in the computational region.

thus assumed to be negligible (i.e. $\partial/\partial x = 0$). On the solid boundary ABCD, the non-slip condition and constant wall temperature apply. To obtain vorticity on the boundary, it is assumed that, in the region near the wall: (1) the property gradients along the wall are zero; and (2) the velocity distribution normal to the wall is linear which leads to a linear variation of vorticity in this region. Integration of the continuity equation,

$$\omega = -\frac{1}{\rho}\nabla^2\psi, \tag{4}$$

gives [6],

$$\omega_w = -\frac{3\psi_1}{(\Delta y)^2\rho} - 0.5\omega_1, \tag{5}$$

where the subscript '1' refers to the node next to the wall and Δy is the distance between this node and the wall node. The wall vorticity expressed in this equation is iterative since ψ_1 varies in each iteration. Because of high gradients of variables near the wall, a very fine grid is utilized in the near wall regions as is described in the next section.

NUMERICAL PROCEDURES

The system of governing differential equations with the boundary conditions is solved using the finite-difference scheme that involves the iterative solution algorithm described in refs. [6] and [8]. In this scheme, the methods of upwind difference and central difference are applied, respectively, to the convective term and to the diffusion term. It is found that the numerical solutions are sensitive to the size of the region ABCDEF (Fig. 1b) as well as to the grid distribution. Considerable effort has been directed to the study of their effect. First, several region sizes are tested using a given grid distribution. The final size is selected after no significant change is observed in the solution. Next, tests of various non-uniform grid systems are made and a choice of the final grid distribution, 31×30, showing grid independency is adopted. The grids as shown in Fig. 1b are finer near the corner and the surface. The finest grid, of dimension $0.025s$, is located adjacent to the wall, and the sizes of other grids are chosen such that each is within 150% of the next grid [6] in order to avoid abrupt changes and to obtain convergence.

In the present algorithm, the Gauss–Seidel iteration scheme is applied for obtaining convergence of each variable. The variable ϕ is said to be convergent if its residual is smaller than a pre-assigned value. The residual is defined as,

$$\beta = |(\phi^n - \phi^{n-1})/\phi^n|_{\max} \tag{6}$$

where n refers to the nth iteration. In the above expression, the residual β represents the maximum value throughout the computational region. The preassigned value is 10^{-3} for all cases except those for the smallest step ($s = 0.38$ cm) for which a value of 10^{-4} is used, since the latter value is found necessary to assure agreement of the computed results with experiments.

It is noted that the governing equations for ψ and ω and the energy equation are uncoupled. The ψ and ω equations are first solved and their results stored. The stored information is then used to obtain the solution of the energy equation. The computation is performed on a VAX11/750 computer. Due to the fine grid system and the relatively complicated computational region, 400–800 iterations are needed for convergence of ψ and ω. On the other hand only 200 iterations are needed to get the temperature solution. In some runs, there are two or three nodal points in the computational region where residuals of ψ and ω still fluctuate in an irregular pattern after 800 iterations. More iterations are then performed to meet the convergence criterion. The resulting converged values however are not noticeably different from the values prior to the additional iterations.

In earlier phases of the computation, the manner to specify the vorticities on the north boundary FE and at the corner B is checked. Along FE, which is neither a wall boundary nor a streamline, one may prescribe $\omega = 0$ or, alternatively, compute ω from equation (4). The result of the computation gives $\omega = -O(10^{-5})$. The use of $\omega = 0$ is therefore adjudged adequate. To obtain the vorticity at the corner B, several averaging methods using the value of its neighboring nodes are tested. The calculated reattachment distance (L/s) varies within 5%. The final choice of the computation is based on the linear relation with the north node next to the corner [6]. In addition, the vorticity at the node point next to the corner in the downstream direction was calculated from equation (4) when the stream function value at this point is assumed to be the corner node value, i.e. ($\psi = 0$).

RESULTS

The computational results for the region ABCDEF in Fig. 1b are presented in this section. In order to afford comparison with the experimental data in [2], results have been obtained primarily for step sizes $s = 1.27$ cm, 0.635 cm and 0.380 cm. Unless otherwise specified, the plate length upstream of the step is $x_s = 45.5$ cm.

The qualitative flowfield

The qualitative flowfield in back step flow has been described by other investigators; here we focus on results that are helpful in investigating the experimental data reported in the recent paper by Aung [2]. Figure 2 shows a contour plot of the dimensionless stream function that is representative of the results obtained in the present study. In the shear layer, streamlines are densely packed, a result of the rapid change of the velocity with distance. The dividing streamline ($\psi = 0$) is not shown, but the reattachment point (L) is indicated. The center of circulation is situated at a location closer to the step than to the reattachment point, being at roughly 25% of the reattachment distance from the step. The streamlines outside of the recirculation region are nearly parallel to each other; however, except for a short distance following the step,

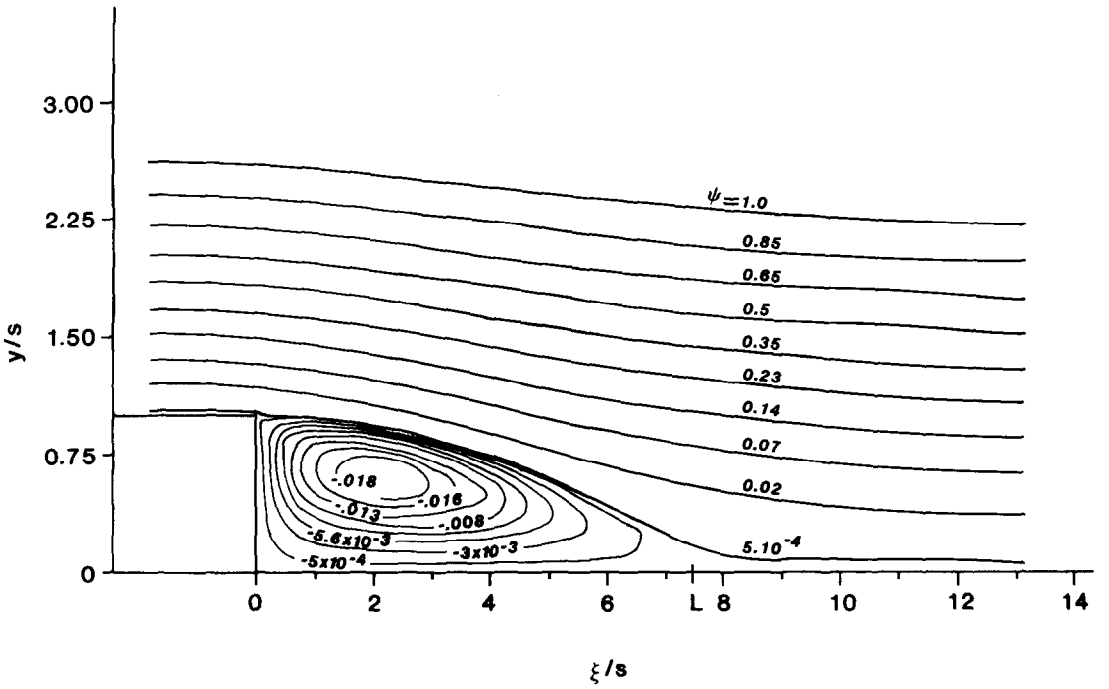

FIG. 2. Streamline distribution for $s = 12.7$ mm and $Re_s = 233$.

the streamlines are not parallel to the upstream wall, as is more likely the case in cavity flow [4].

The above qualitative pattern is maintained for all steps and at all Reynolds numbers. At a given step size, an increase in the velocity and hence the Reynolds number elongates the separation bubble, accompanied by an increase in the reattachment distance.

A close examination of the streamline plots reveals that the dividing streamline, which separates the downstream flowing fluid from that which reverses, does not originate at the upper corner of the step. Instead, the streamlines immediately adjacent to the upstream wall appear to dip suddenly upon passing the step, so that the dividing streamline originates at some distance below the upper corner of the step. The streamline deflection at the step is very minute, with the depression of the dividing streamline amounting to no more than 1% of the step height in the cases studies.

There are two additional noteworthy points. One is that most streamlines in the shear layer, in general, proceed for some distance beyond the step in a direction approximately parallel to the downstream step wall. (Note that the axial distance has been compressed in Fig. 2.) The same observation has been made in [2] based on preliminary evidence in flow observation. The second point deals with the comparison with laminar flow in a cavity. Numerical computations using two different calculational approaches, one based on the stream function–vorticity formulation and completed by Jacobs and Sutton [9] and the other by Bhatti and Aung [4] using the primitive variables of u, v, and p, show that in certain instances of laminar flow past a rectangular cavity, the dividing streamline bulges out slightly towards the external flow. Such a phenomenon is caused by the relatively strong vorticity in the comparatively more confined space of a cavity. In the backstep problem, the recirculation is bounded only on two sides by solid walls, so that the transverse stretching or bending of the streamlines in the shear layer is not as noticeable.

Figure 3 shows the dimensionless vorticity distributions for the step size, $s = 12.7$ mm. It is seen that the vorticity which is very strong near the corner of the step is swept and transported into the recirculation region. In addition, the decay of vorticity in the transverse direction is rather fast. Within the recirculation region, the value of the vorticity changes sign when one follows a closed streamline. There is an influence of Reynolds number on the vorticity distributions for a fixed step size (not shown in the figure), i.e. an increase in Reynolds number leads to an increase in the vortex strength. This is because the Reynolds number increase designates an increase in the velocity which in turn means a smaller boundary-layer thickness at the step (i.e. a smaller initial shear-layer thickness). Thus, a smaller initial thickness gives rise to higher vorticity values in the separated region. Larger vorticities lead to vortices of higher strengths and therefore to higher heat transfer in the recirculation zone. Hence, heat transfer increases with the Reynolds number.

The proximity of the downstream wall exerts a strong effect on the transport of vorticity. Consider Figs. 4a and 4b that display isovorticity plots for various step

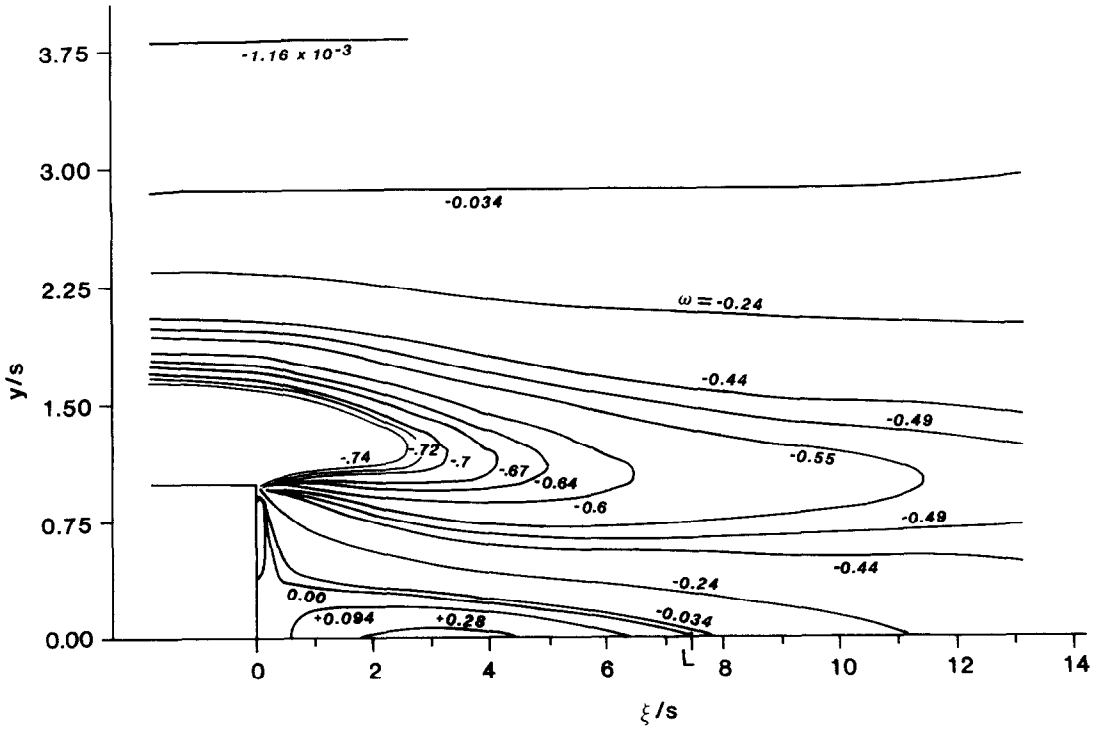

FIG. 3. Vorticity distribution for $s = 12.7$ mm and $Re_s = 233$.

sizes at a Reynolds number of approx. 200. Note that the velocity is higher and the initial shear layer is thinner when the step size is smaller, in order to give the same Reynolds number. Even then, there is a smaller vorticity transport into the region behind the step, when the step size is reduced. This explains why in ref. [2], it is observed that the overall heat transfer in separated flow decreases as the step size is reduced.

Reattachment length

By closely examining the computed stream function results, the location where the dividing streamline meets the downstream wall may be ascertained. Existing literature indicates that the reattachment distance is related to the system and flow parameters in a rather complicated way; this is confirmed by the results obtained in the present study. Figure 5 indicates

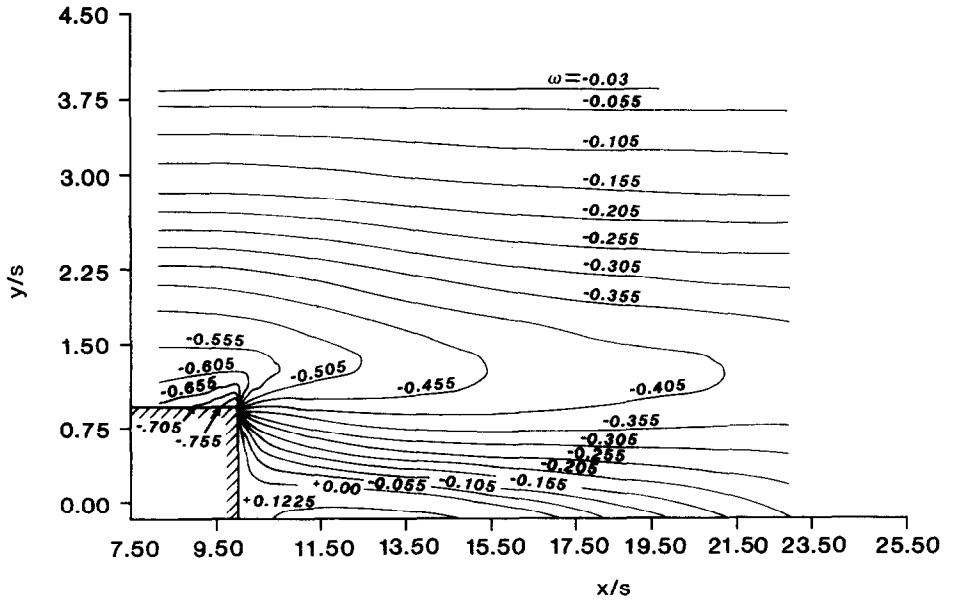

FIG. 4a. Vorticity distribution for $s = 6.35$ mm and $Re_s = 200$.

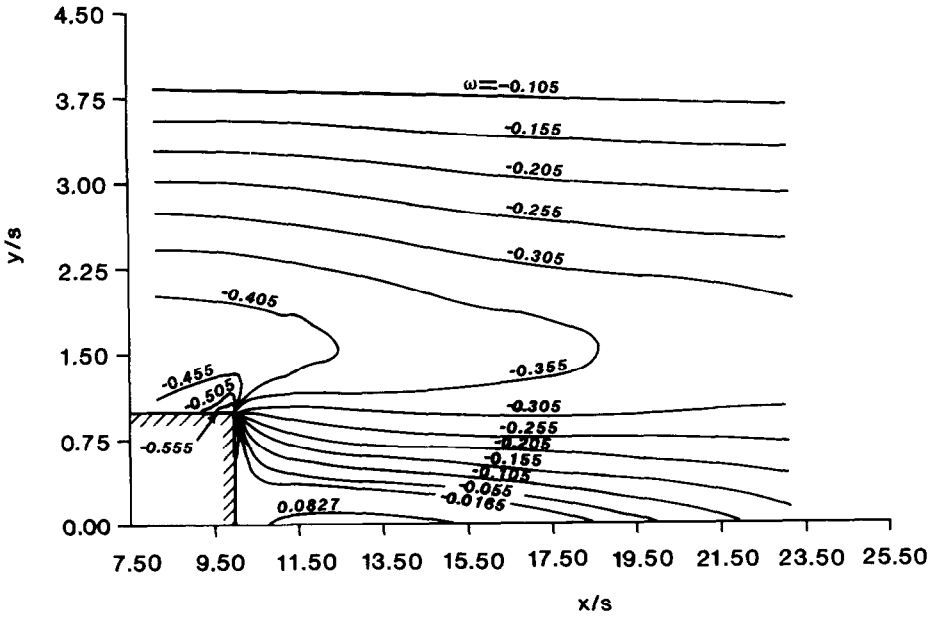

FIG. 4b. Vorticity distribution for $s = 3.80$ mm and $Re_s = 206$.

the normalized reattachment lengths as a function of the Reynolds number. As expected, the calculated results cannot be represented by a single curve. Furthermore, the relationship between L/s and Re_s is not a linear one for any given step. In fact, the rate of increase of the dimensionless reattachment distance is greater at lower values of the Reynolds number. The curves also seem to intersect in the lower range of the Reynolds number; however, the slopes of the curves for all steps appear to be nearly the same when the Reynolds number is larger than about 180.

Figure 5 also contains the experimental data of Goldstein *et al.* [10], Leal and Acrivos [11], and of Aung [2]. In general, the present computation yields

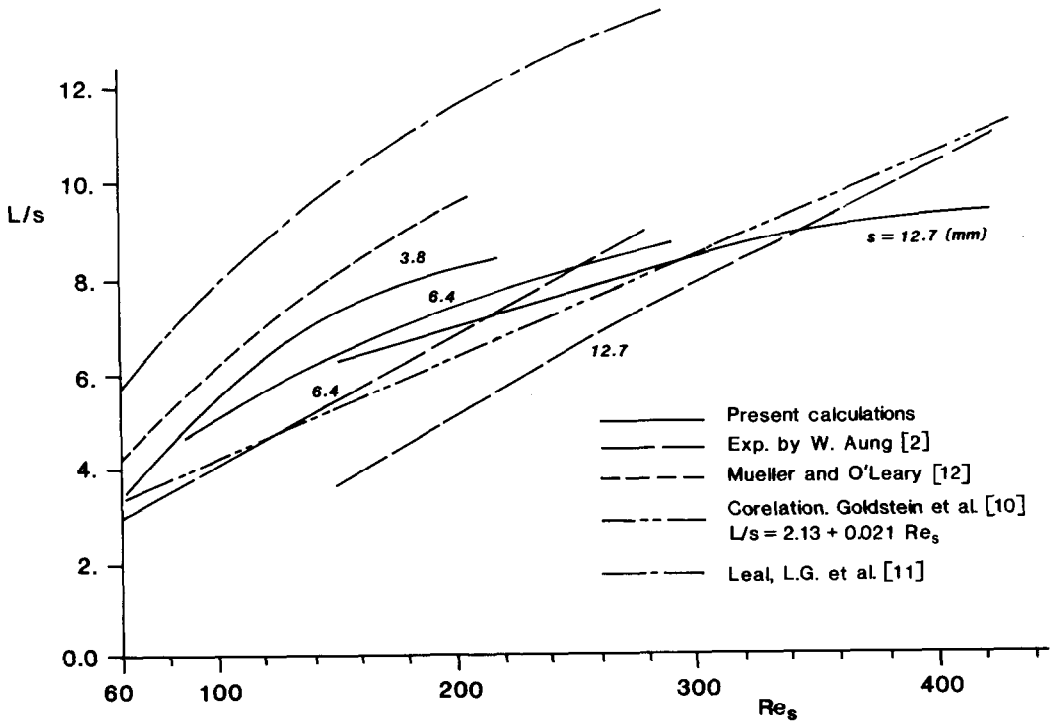

FIG. 5. Reattachment length vs Re_s.

results that are higher than the experimental data in the lower Reynolds number range. This is consistent with the calculated results of Mueller and O'Leary [12] which are also displayed in Fig. 5. At the higher end of the Reynolds number range, the experimental measurements give data that are larger than the present computed results. No fully satisfactory explanation is forthcoming at this time, but the disparity of the various results shown in this figure certainly underscores the variability of the reattachment distance to system and flow variables, such as step and initial shear-layer dimensions. The effect of the initial shear-layer thickness has been investigated in the present study and will be discussed shortly. It should be emphasized that a comparison based on the reattachment length represents a very stringent test of the experimental accuracy or numerical stability. Yet, the locality of the reattachment point usually has large heat transfer rates; hence an error in pinpointing the reattachment location can lead to significant errors in estimating an average heat transfer in the recirculation region. This is an area that deserves to be examined more carefully. In addition to variables due to the system and to the flow, differences in the experimental and numerical approaches could also be responsible for the variability of the results. In this regard, it may be noted that the computational procedure used in the present investigation is known to be conservative. The presence of false diffusion could very well be the reason that the present approach leads to larger dimensionless reattachment distances as compared with experimental data over most of the Reynolds number range of interest here; however, as noted previously great care was exercised in the present study to ensure grid-independence of results, and false diffusion has been minimized to the extent possible. It is also recalled that the measurements in refs. [2, 10] were conducted using uncooled cigar smoke introduced into a cold flow tunnel in which the step geometry formed a part of the top wall. It is therefore an inverted step and buoyancy effects could have caused the relatively hot smoke filaments to reattach closer to the step. It is also noted that the present calculated results fall between the Mueller and O'Leary curve and the experimental data of refs. [2, 10].

In order to assess the influence of the initial shear-layer thickness on the reattachment length (and indirectly on the heat transfer), the following methods are chosen in the present study. First, at a given step size, a Reynolds number is chosen and held fixed (i.e. the freestream velocity is fixed). Then by varying the hypothetical flat plate length upstream of the line AF in Fig. 1b, velocity profiles with varying boundary-layer thicknesses are specified on AF. The boundary-layer thicknesses at the step are then obtained from the solutions. In each case, the thickness at the step is smaller than the value specified on AF. The reason is that the curvature effect caused by the step gives rise to a thinning of the boundary layer. For the cases studied herein, Table 2 gives the values for input displacement

Table 2. Boundary-layer displacement thicknesses and reattachment distances

	Re_s	x_s (mm)	L/s	δ^*_{AF}/s	δ^*_{FP}/s	δ^*/s
	63	755	3.451	2.994	3.072	2.974
	⋮	455	3.584	2.283	2.385	2.262
	⋮	305	3.590	1.827	1.953	1.798
	110	1100	5.944	2.758	2.805	2.740
	⋮	750	5.691	2.258	2.317	2.236
	⋮	600	5.586	2.006	2.073	1.982
$s = 3.8$ mm	⋮	455	5.487	1.728	1.805	1.700
	⋮	305	5.407	1.383	1.478	1.335
	206	750	8.995	1.650	1.697	1.613
	⋮	455	8.108	1.280	1.337	1.233
	⋮	380	7.861	1.143	1.205	1.111
	⋮	190	7.248	0.762	0.852	0.727
	⋮	76	6.820	0.381	0.539	0.331
	200	750	7.941	1.272	1.329	1.241
	⋮	455	7.326	0.961	1.035	0.928
	⋮	318	7.151	0.774	0.865	0.738
$s = 6.35$ mm	⋮	127	6.740	0.387	0.547	0.337
	⋮	1100	10.337			1.296
	272	755	9.389	1.095	1.144	1.060
	⋮	455	8.529	0.824	0.888	0.791
	⋮	305	8.116	0.647	0.727	0.610
	209	1000	7.639	0.992	1.062	0.958
	⋮	635	7.296	0.757	0.846	0.722
	⋮	455	7.109	0.608	0.716	0.595
$s = 12.7$ mm	⋮	318	6.931	0.463	0.598	0.419
	315	1100	9.483	0.853	0.907	0.811
	⋮	755	8.862			0.635
	⋮	455	8.294	0.495	0.583	0.449
	⋮	305	8.035	0.365	0.478	0.328

thickness (on AF), δ^*_{AF}; the flat plate (Blasius) thickness, δ^*_{FP}, that would be obtained at the step if the step size were set equal to zero; and the computed thickness at the step, δ^*.

The results of the computation are indicated in Fig. 6. The influence of the boundary-layer thickness is most pronounced at the highest Reynolds numbers. As the Reynolds number is reduced, so is the slope of the curve. When the Reynolds number is nearly the same, the curves are almost identical; this is exhibited by the lines *C*, *D*, and *E*, which represent three different steps, but the Reynolds number is approximately constant (about 200). At a Reynolds number of 110, the slope is very small but is still positive. At the least value of the Reynolds number studied the slope, while small, has become negative. It is noteworthy, however, that in all other Reynolds numbers, the slope is positive. Therefore, in most practical situations, an increase of the initial shear-layer thickness elongates the axial extent of the separation bubble.

The second method used for assessing the effect of the initial shear-layer thickness is as follows. We assume that the length of the upstream plate, x_s, is fixed and is equal to 45.5 cm. Then, for a given step size, the Reynolds number and hence the free-stream velocity is varied until a desired displacement thickness is obtained at the input boundary AF. A solution for the flowfield is then obtained as before giving the value of the displacement thickness at the step and the corresponding reattachment distance. Normalized values of these quantities are plotted in Fig. 7 for four step sizes. The curves indicate a strong dependency of the reattachment distance on the boundary-layer thickness. Inherent in the inter-relationship displayed in the figure is the effect of the free-stream velocity, which must be reduced to increase the boundary-layer thickness.

Figures 6 and 7 show trends that are by and large opposite, and suggest the need to exercise care while considering the influence of the upstream boundary layer. Clearly, changes in the boundary-layer thickness cannot be divorced at all times from free-stream velocity changes, and the effects of these two parameters are sometimes intermingled.

Velocity and temperature profiles

Streamwise velocities have been evaluated from stream function solutions, and typical results are

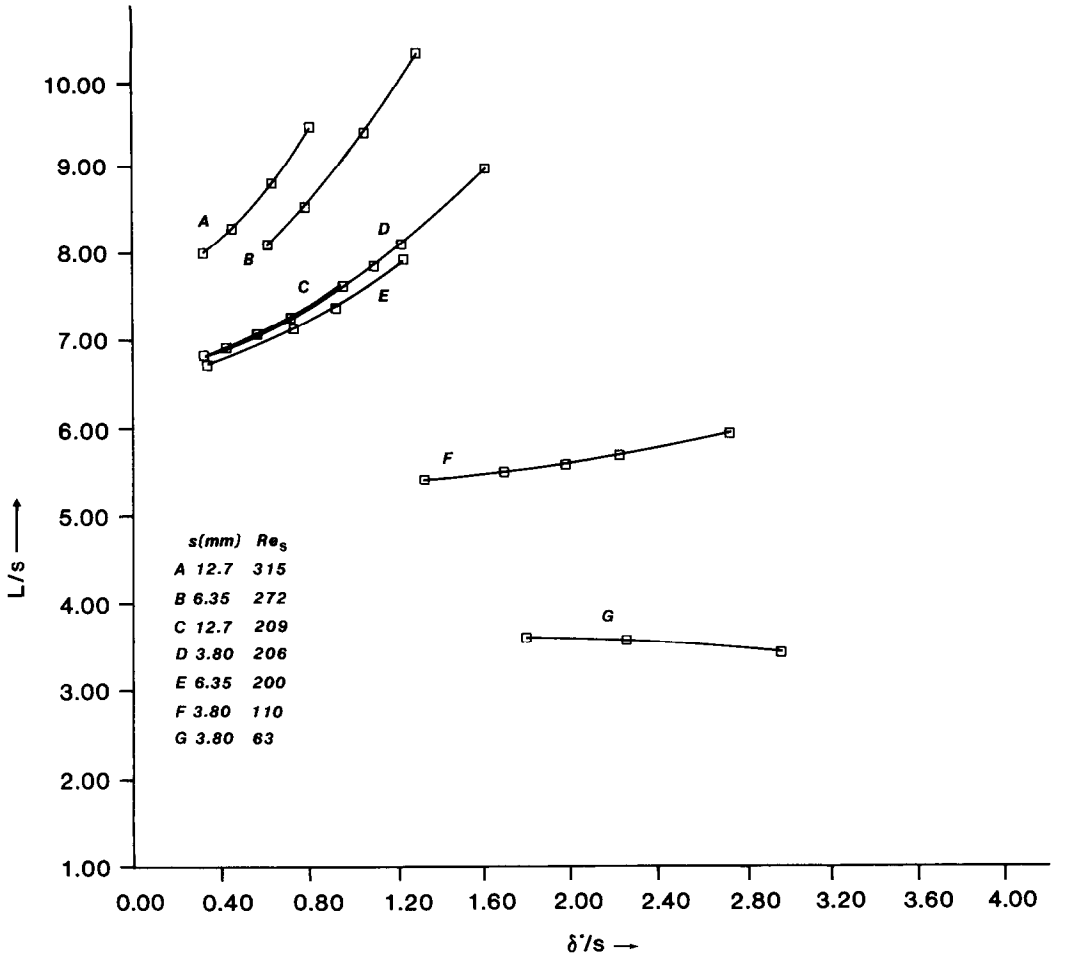

FIG. 6. Reattachment distance vs displacement thickness at the step ($x_s/s \neq$ constant).

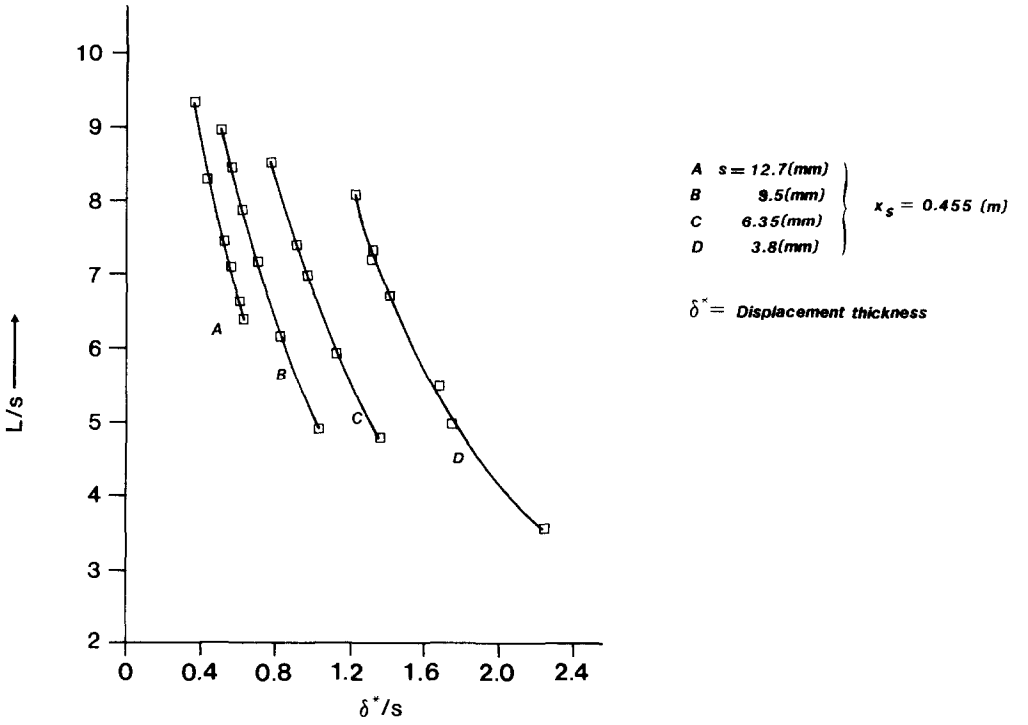

FIG. 7. Reattachment distance vs displacement thickness at the step ($Re_s \neq$ constant).

plotted in Fig. 8a for the step size of 12.7 mm at a Reynolds number of approx. 200. The reverse flow velocity is significant, amounting to roughly 7% of the free-stream velocity.

In a recent paper [2], it was shown that the average heat transfer in the separated region can be predicted using the wall-independent shear-layer analysis reported in [3]. The latter analysis is primarily focused on the separated shear layer, which is assumed to originate at the point of separation with zero thickness. The wall underneath the shear layer is considered remote from it. Boundary-layer approximations are then applied to the momentum equations, and a similar procedure is used to solve the energy equation. The ensuing solutions for the shear layer are related to the total wall heat transfer by means of an integral energy balance. It is of interest to compare and contrast the velocity profiles of the present calculations with those given by the theory in [3], which admits of no reverse flow. In specializing the dimensionless analytical velocity profiles derived in [3] to the present problem involving a shear layer with a finite thickness prior to separation, it is assumed that the shear layer originates at the leading edge of the hypothetical plate upstream of the step. The theoretical velocity profiles thus generated are compared with the profiles obtained in the present numerical solutions in Fig. 8a. The similarity variables used in [3] are employed, and the results are shown for several streamwise locations in the separated region. The corresponding temperature distributions are indicated in Fig. 8b. In view of the simplifying assumptions inherent in the similarity analysis, the discrepancies between it and the present numerical results are not surprising. The aim here, however, is to observe how the discrepancy changes with step size. The study in [2] shows that the wall-independent shear-layer theory becomes more accurate as the step size becomes larger. The present figures show that the velocity and temperature distributions for the wall-independent shear-layer theory also more closely approaches the numerical results when the step size is greater. As indicated in one of the following sections, the present numerical solutions represent the physical situation quite closely.

It may be noted from Figs. 8a and b that the wall-independent shear-layer theory still deviates substantially from the real situation even at the largest step size studied. Hence, the close agreement of the theory with the experiments for this step size [2] must be because of the unimportance of detailed profile shapes. This lends further credence to approximate approaches, such as embodied in the wall-independent theory, in the study of separated forced convection, but these approaches must account for the initial shear-layer thickness.

Local Stanton number distributions

Figure 9 shows typical variations of the local heat transfer downstream of the step. The numerical results are expressed in the form of the Stanton number. The local heat transfer for both cases grows rapidly from the corner of the step, eventually levels off and then decreases. At large distances from the step, the

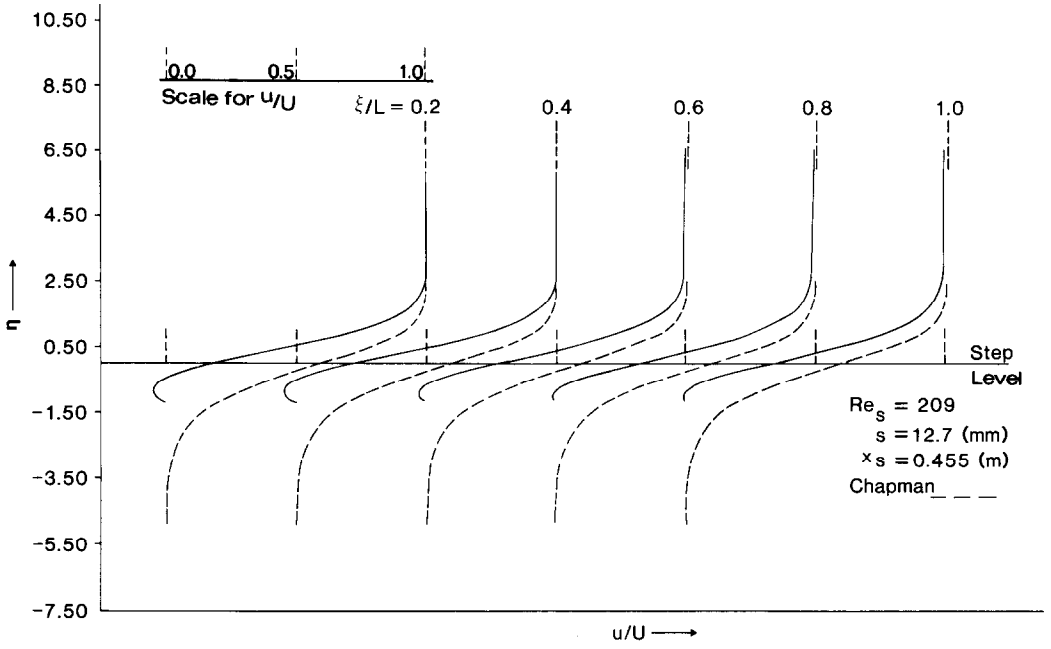

FIG. 8a. Flow velocity vs similarity variable [$\eta = 1/2(y-s)\sqrt{U/vx}$].

streamwise variation of the heat transfer appears to assume the trend of the variation on the hypothetical flat plate that would be obtained by setting the step size to zero.

The wall-independent shear-layer analysis [3] indicates that, in laminar flow, the average heat transfer is reduced to 56% of the attached flow value. Experiments reported in [2] show that the average heat transfer is reduced, but the amount of reduction depends on the step size, being smaller for a larger step; and that the local heat transfer is less than the hypothetical flat plate value. The numerical results shown in Fig. 9 qualitatively confirm the experimental trends. Despite the similar trends for the streamwise variation of the local Stanton number for the two step sizes, there is a significant difference, which is that while the Stanton number for $s = 1.27$ cm eventually merges with the flat plate curve, that for $s = 0.38$ cm appears to

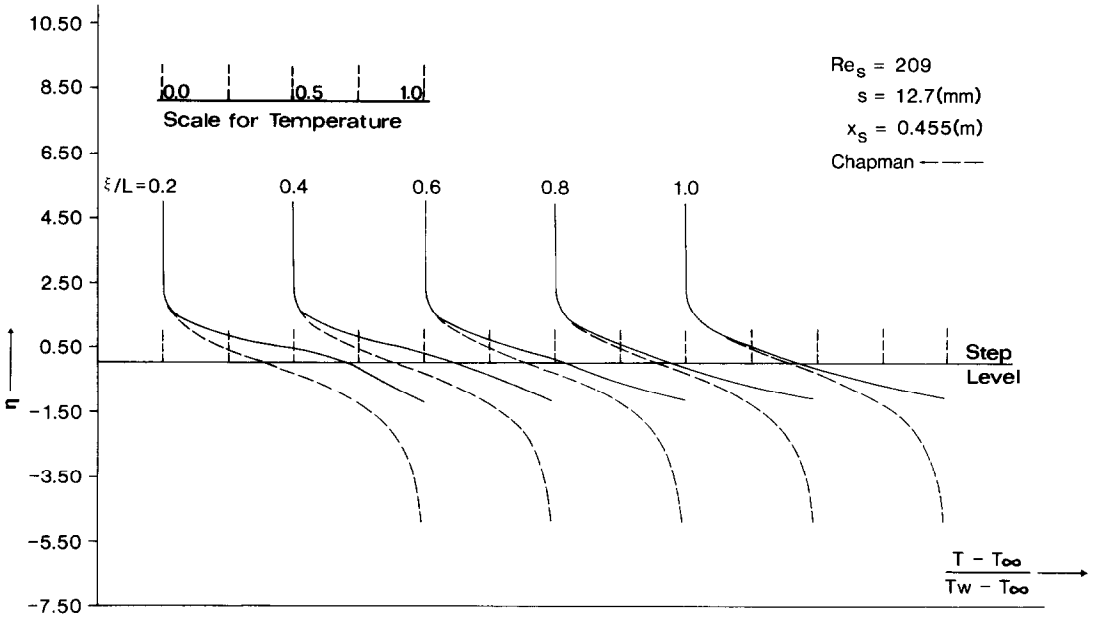

FIG. 8b. Temperature distribution vs similarity variable [$\eta = 1/2(y-s)\sqrt{U/vx}$].

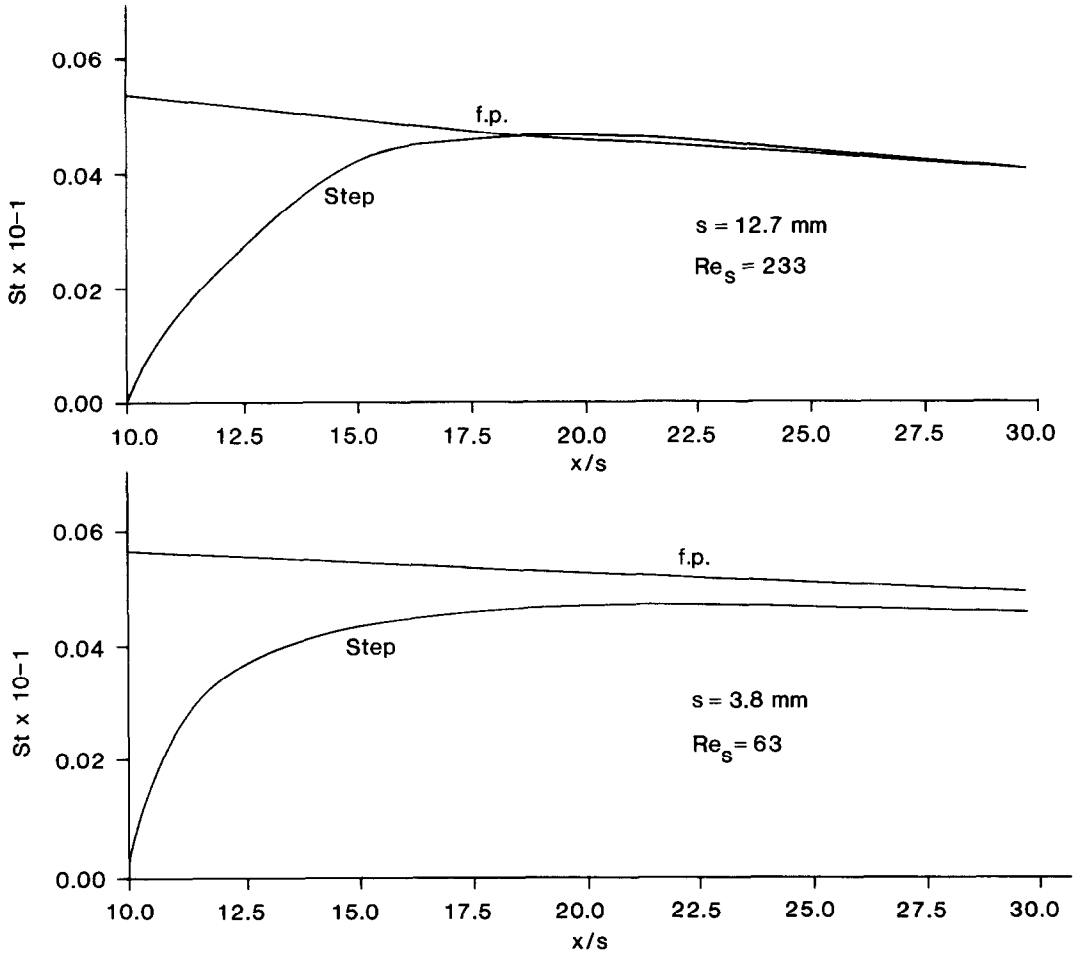

FIG. 9. Local Stanton number for $s = 12.7$ mm and $s = 3.8$ mm.

suffer a permanent deficit. In fact, as is clear from [2], the deficit becomes larger as the step gets smaller. The correlation given in [2] shows that the average Stanton number in the recirculation zone is inversely proportional to the upstream plate length (normalized by the step size) raised to the -0.72 power. The specific relation given in [2] is:

$$\overline{St} = 0.787(Re_s)^{-0.55}\left(\frac{s}{x_s}\right)^{0.72}. \tag{7}$$

The above equation may be combined with the relations for the thicknesses of the laminar boundary layer, as given by Kays and Crawford [13]. Written for the boundary-layer thicknesses at the step, these relations are:

$$\frac{\delta_{FP}}{x_s} = 4.64/(Re_{x_s})^{0.5} \tag{8}$$

$$\frac{\delta^*_{FP}}{x_s} = 1.73/(Re_{x_s})^{0.5}. \tag{9}$$

Hence,

$$\frac{\delta_{FP}}{\delta^*_{FP}} = 2.68. \tag{10}$$

From equations (7) and (8), the following expression for the average heat transfer in the recirculation zone may be derived:

$$\overline{St} = 0.787(Re_s)^{0.17}\left(\frac{\delta_{FP}}{s}\right)^{1.44}. \tag{11}$$

By means of equations (10) and (11) an expression giving the influence of the displacement thickness may be obtained.

Equation (11) shows that the average Stanton number depends rather strongly on the initial shear-layer thickness. In deriving it, it has been assumed that equation (8) is valid at the step, which is not exactly true as may be seen from Table 2. The latter indicates that in all cases, $\delta_{FP} > \delta$.

Comparison with experiments

The data in [2] indicate that for any given step, the local heat transfer in the separated region may be collapsed into nearly a single curve when plotted as:

$$\frac{Nu}{\sqrt{Re_s}} = f\left(\frac{\xi}{L}\right). \tag{12}$$

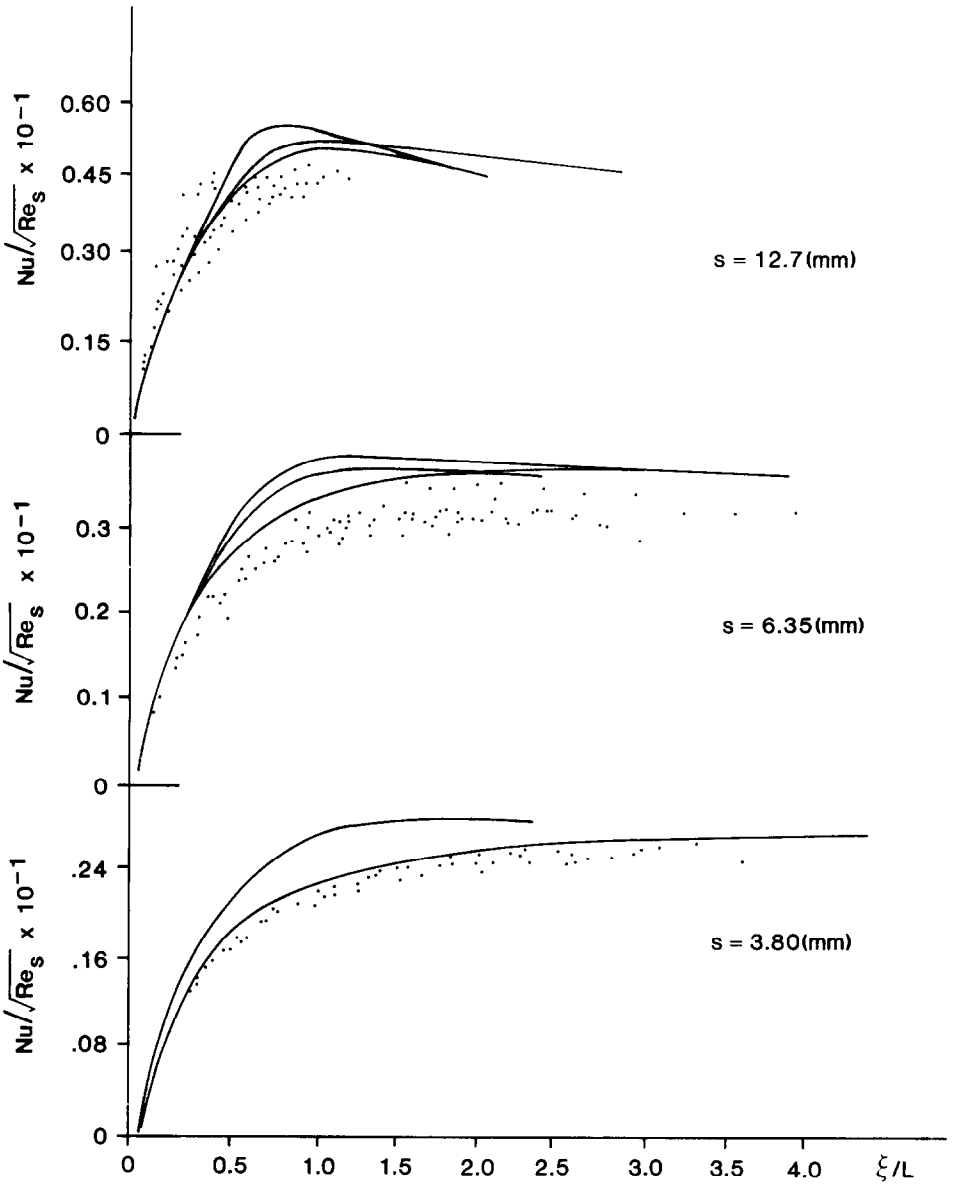

FIG. 10. Comparison of the computed $Nu/\sqrt{Re_s}$ with the experimental values.

Figure 10 indicates the numerical calculations together with the experimental data from [2]. It is clear from the figure that the coordinates selected for the graphs do not lead to a perfect correlation at any of the step sizes investigated. When a larger step is involved, the spread among the curves for the various Reynolds numbers is less for the numerical solutions than for the physical experiments, but the trend is reversed when a smaller step is considered. Obviously, a more complicated functional relation than that given in equation (12) must be considered.

The computed temperature distributions are plotted at several streamwise locations and compared in Fig. 11 with the profiles [2] measured by means of a Mach–Zehnder interferometer. Here, the agreement between the theoretical and experimental profiles is much closer than that based on the evaluation of the temperature gradients as is involved in obtaining Fig. 10.

CONCLUSION

The present theoretical analysis of the flow and heat transfer in laminar flow past backsteps has made it possible to examine for the first time a number of factors which are important in such flows. The initial shear-layer thickness is shown to influence the flow and heat transfer in a number of ways. A smaller initial thickness, in general, is shown to lead to higher vorticities and hence to higher heat transfer in the separated region, when the step size is held fixed and shear-layer thickness is allowed to change as the velocity and hence the Reynold number is changed. The influence of the initial

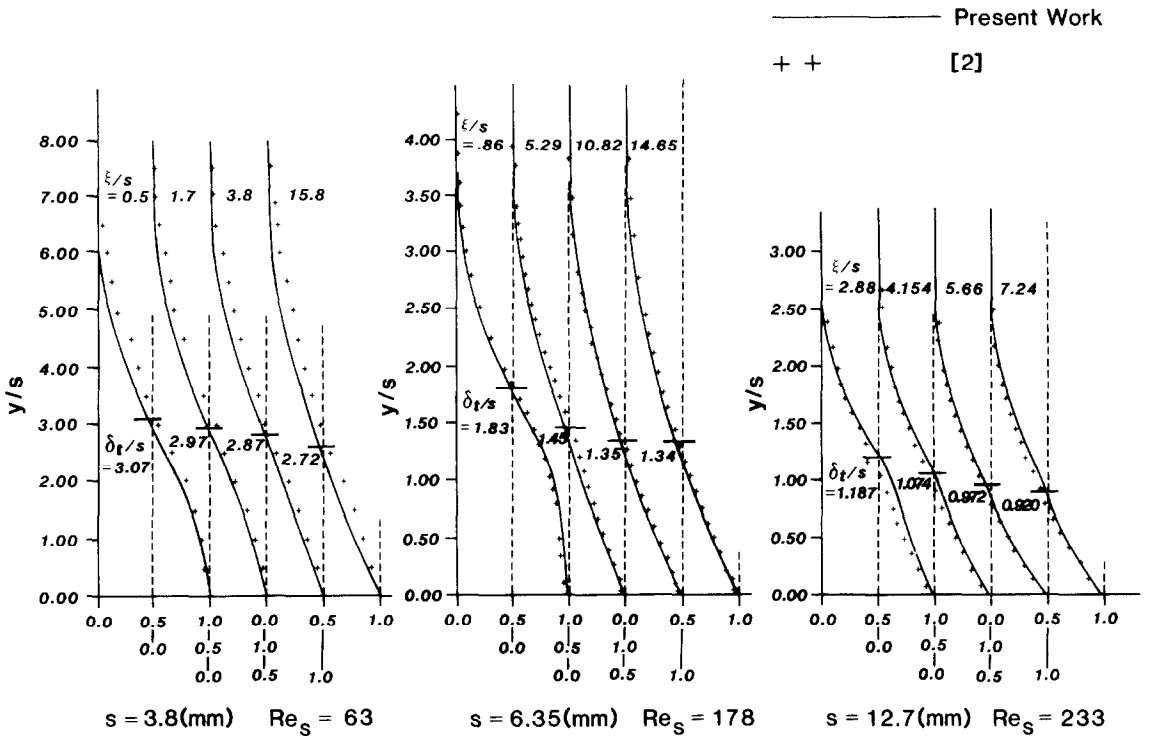

FIG. 11. Temperature profiles for the steps showing comparison with experimental data from [2].

shear-layer thickness on the reattachment distance is shown to depend on how this thickness is varied. For a given step size, the shear-layer thickness can be altered either by keeping the free-stream velocity fixed (hence the Reynolds number is fixed) and changing the dimension of the upstream plate, or by keeping the upstream plate fixed and varying the velocity (thereby changing the Reynolds number). In the first case, the reattachment distance is shown to increase as the initial shear-layer thickness grows, but the rate of increase slows as the Reynolds number is held constant at smaller values and in fact becomes negative at the smallest Reynolds number investigated. In the second case, the reattachment distance increases as the initial shear-layer thickness decreases in each of the step sizes studied.

Previous experimental data indicate that the average Stanton number in the separated region is related to the Reynolds number in a functional form as predicted by the simple wall-independent shear-layer theory. A comparison of the velocity and temperature profiles computed in this study and those given by the simple theory indicates major discrepancies in the separated region. This shows the relative unimportance of the details of the near-wall flow and thermal structures insofar as the average heat transfer is concerned.

REFERENCES

1. W. Aung, Separated forced flow, *Keynote Speeches, ASME/JSME Thermal Engineering Joint Conference Proceedings*, Vol. 2, pp. 449–515. Honolulu, Hawaii (March 1983).
2. W. Aung, An experimental study of laminar heat transfer downstream of backsteps, *J. Heat Transfer* **105**, 823–829 (1983).
3. D. R. Chapman, A theoretical analysis of heat transfer in regions of separated flow, NACA TN 3792 (1956).
4. A. Bhatti and W. Aung, Finite difference analysis of laminar separated forced convection in cavities, *J. Heat Transfer* **106**, 49–54 (1984).
5. E. J. Hall and R. H. Fletcher, Application of a viscous–inviscid interaction procedure to predict separated flows with heat transfer, ASME paper 83-WA/HT-7.
6. A. D. Gosman, N. M. Pan, A. K. Punchal, D. B. Spalding and M. Wolfstein, *Heat and Mass Transfer in Recirculating Flows*. Academic Press, New York (1969).
7. E. R. G. Eckert and R. M. Drake, *Analysis of Heat and Mass Transfer*. McGraw-Hill, New York (1972).
8. F. Huang and F. K. Tsou, Friction and heat transfer in laminar free swirling flow in pipes. In *Gas Turbine Heat Transfer*, pp. 71–78. American Society of Mechanical Engineers (1978).
9. H. R. Jacobs and S. B. Sutton, A numerical study of cavity flows with and without mass addition, heat transfer. *Proc. 5th Int. Heat Transfer Conference*, Vol. 2, pp. 40–44, Tokyo, Japan (1974).
10. R. J. Goldstein, V. L. Eriksen, R. M. Olson and E. R. G. Eckert, Laminar separation, reattachment and transition of flow over a downstream facing step, *Trans. Am. Soc. mech. Engrs, J. bas. Engng* **92**, 732–741 (1970).
11. L. G. Leal and A. Acrivos, The effect of base bleed on the steady separated flow past bluff objects, *J. Fluid Mech.* **39**, 735–752 (1969).
12. T. J. Mueller and R. A. O'Leary, Physical and numerical experiments in laminar incompressible separating and reattaching flow, AIAA Paper No. 70-763 (1970).
13. W. M. Kays and M. E. Crawford, *Convective Heat and Mass Transfer*, 2nd edn. McGraw-Hill, New York (1980).

INDEPENDANCE DE PAROI ET EFFET DE L'EPAISSEUR INITIALE DE LA COUCHE CISAILLEE DANS UN ECOULEMENT SEPARE ET TRANSFERT THERMIQUE

Résumé—On présente des résultats théoriques concernant l'écoulement et le transfert de chaleur dans un écoulement laminaire en aval d'une marche. Des calculs sont conduits en utilisant fonction de courant–vorticité dans les équations aux dérivées partielles elliptiques. Les effets de la dimension de la marche et de l'épaisseur initiale de la couche cisaillée sont discutés; les profils de température et les nombres de Stanton locaux sont comparés avec des données expérimentales récentes. On montre que la taille de la couche limite initiale peut avoir des effets opposés sur la distance de réattachement, dépendant du nombre de Reynolds maintenu constant. L'influence sur le transfert thermique moyen et sur les structures thermiques dans la région de l'écoulement de retour est dégagée en comparant les solutions numériques avec les solutions relatives à la couche de cisaillement indépendante de la paroi.

WANDUNABHÄNGIGKEIT UND EINFLUSS DER ANFÄNGLICHEN SCHERUNGSSCHICHTDICKE BEIM WÄRMEÜBERGANG IN EINER ABGELÖSTEN STRÖMUNG

Zusammenfassung—Es werden theoretische Ergebnisse bezüglich der Strömung und des Wärmeübergangs in einer laminaren Strömung nach einer plötzlichen Erweiterung vorgestellt. Die Berechnungen werden unter Verwendung der Stromfunktion-Wirbeltransport-Form der elliptischen partiellen Differentialgleichungen durchgeführt. Die Einflüsse der Stärke der Erweiterung und der anfänglichen Grenzschichtdicke werden diskutiert und berechnete Temperaturprofile und örtliche Stanton-Zahlen mit kürzlich veröffentlichten Meßergebnissen verglichen. Es wird gezeigt, daß die Dicke der anfänglichen Grenzschicht gegensätzliche Einflüsse auf die Länge bis zum Wiederanlegen haben kann, abhängig davon, ob die Reynolds-Zahl konstant gehalten wird. Der Einfluß auf den mittleren Wärmeübergang der Strömung und die thermischen Strukturen im Rückströmgebiet wird durch Vergleich der numerischen Lösungen mit den Lösungen für die wandunabhängige Scherungsschicht abgeschätzt.

НЕЗАВИСИМОСТЬ ОТ СТЕНКИ И ВЛИЯНИЕ НАЧАЛЬНОЙ ТОЛЩИНЫ СДВИГОВОГО СЛОЯ НА ДИНАМИКУ И ТЕПЛОПЕРЕНОС В ОТРЫВНОМ ПОТОКЕ

Аннотация—Представлены теоретические результаты по динамике поля скорости и теплопереносу в ламинарном потоке за уступом. Расчеты проведены с использованием эллиптических уравнений в частных производных в форме 'функция тока-завихренность'. Обсуждается влияние размера уступа и начальной толщины пограничного слоя, а рассчитанные температурные профили и локальные числа Стэнтона сравниваются с недавно опубликованными экспериментальными данными. Показано, что размер начального пограничного слоя может оказывать противоположное влияние на точку присоединения в зависимости от того, поддерживается число Рейнольдса постоянным или нет. Влияние на средний теплоперенос динамических и тепловых структур в зоне обратного течения оценивается сравнением полученных численных результатов с соответствующими решениями для независящего от стенки сдвигового слоя.